Pergamon

Bioorganic & Medicinal Chemistry Letters 11 (2001) 711–714

BIOORGANIC & MEDICINAL CHEMISTRY LETTERS

Synthetic Analogues of SB-219383. Novel *C*-Glycosyl Peptides as Inhibitors of Tyrosyl tRNA Synthetase

Pamela Brown,[a,*] Drake S. Eggleston,[a] R. Curtis Haltiwanger,[b] Richard L. Jarvest,[a] Lucy Mensah,[a] Peter J. O'Hanlon[a] and Andrew J. Pope[a]

[a]*GlaxoSmithKline, New Frontiers Science Park, Third Avenue, Harlow, Essex, CM19 5AW, UK*
[b]*GlaxoSmithKline, 709 Swedeland Road, King of Prussia, PA 19406, USA*

Received 29 November 2000; accepted 12 January 2001

Abstract—Novel inhibitors of bacterial tyrosyl tRNA synthetase have been synthesised in which the cyclic hydroxylamine moiety of SB-219383 is replaced by *C*-pyranosyl derivatives. Potent and selective inhibition of bacterial tyrosyl tRNA synthetase was obtained.

Aminoacyl tRNA synthetases perform a crucial role in protein biosynthesis, catalysing the attachment of an amino acid onto its cognate tRNA. Selective inhibition of bacterial isoleucyl tRNA synthetase can be achieved with pseudomonic acid and synthetic analogues, and this gives rise to potent antibacterial activity.[1] In our search for novel inhibitors of bacterial tRNA synthetases as potential antibacterial agents, the natural product, SB-219383 **1**,[2,3] was discovered as a potent, selective inhibitor of bacterial tyrosyl tRNA synthetase (YRS). We have also shown that the bicyclic scaffold is not an essential feature for enzyme inhibition. For example, the monocyclic compound **2**, derived from SB-219383[4] and the synthetic counterpart **3**[5] show equal potency to SB-219383. In addition, the synthesis of **3** has also enabled us to infer the absolute stereochemistry of the natural product and its derivatives. These compounds, however, show only weak antibacterial activity, probably attributable to their high polarity preventing penetration into the bacterial cell. The hydroxylamine moiety is also a potential liability in the structure. We sought to identify a simplified carbohydrate based scaffold that could replace the cyclic hydroxylamine and maintain inhibition of YRS. Here we describe the synthesis of arabinose-derived analogues, one of which exhibits nanomolar levels of inhibition of YRS.

A pyranose template was selected for the initial mimic of the hydroxylamine-containing ring. The few reported syntheses of natural products containing *C*-glycosyl α-amino acids mainly utilise multi-step introduction and unmasking of the amino acid functionality. We wished to use a short synthesis applicable to a variety of

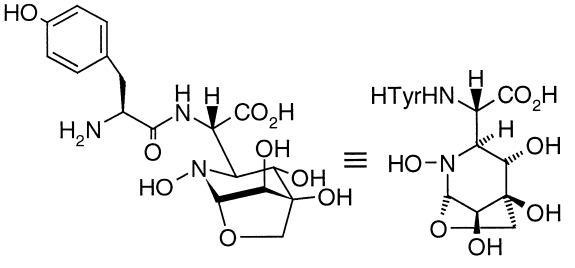

1 SB-219383

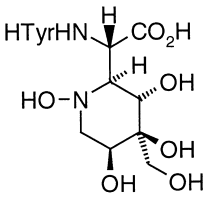

2

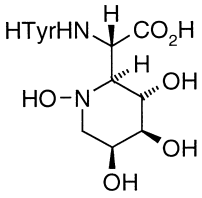

3

*Corresponding author. Tel.: +44-1279-627633; fax: +44-1279-627628; e-mail: pam_brown-1@sbphrd.com

0960-894X/01/$ - see front matter
PII: S0960-894X(01)00039-7

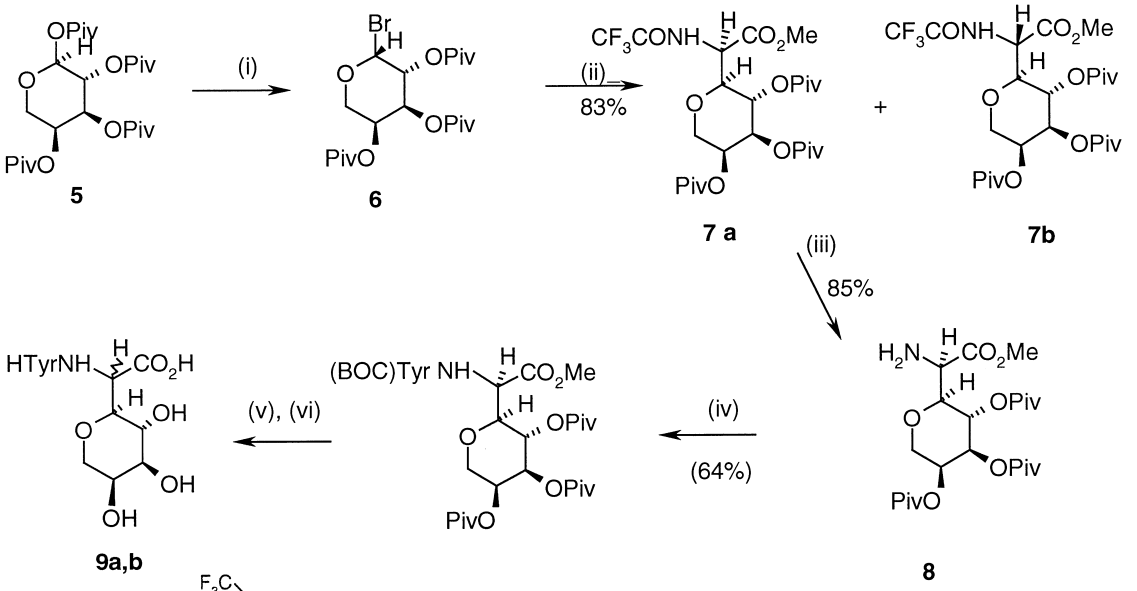

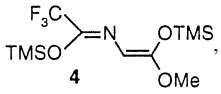

Scheme 1. (i) HBr, HOAc; (ii) 4, $ZnBr_2$, 1,2-dichloroethane, reflux, 18 h; (iii) $NaBH_4$, MeOH, 0 °C–rt, 1.5 h; (iv) BOCTyr, 1-hydroxybenzotriazole, EDAC, DMF, $N(^iPr)_2Et$, 18 h; (v) NaOMe, MeOH, 16 h; (vi) TFA.

templates, and decided to adopt a *C*-glycosylation strategy in order to introduce the glycine unit in one step. Lewis-acid promoted nucleophilic addition has been a fruitful source of *C*-glycosylated sugars.[6] In one example,[7] the silyl ketene acetal **4** derived from glycine,[8] has been reported to react with a glucopyranoside system, although the protected amino-acid moiety was not elaborated further. Our development and extension of this methodology as applied to L(+)-arabinose is shown in Scheme 1.

L(+)-Arabinose was converted to the tetrapivaloyl derivative **5** in 34% yield, and the structure confirmed by X-ray crystallography. Compound **5** was converted into the anomeric bromide **6**, and allowed to react with the silyl ketene acetal **4** derived from *N*-trifluoroacetyl glycine methyl ester using zinc bromide as Lewis acid catalyst to afford the *C*-glycosylated product **7** as a 1:1 mixture of diastereomers at the glycine centre. The diastereomers were separable by column chromatography. X-ray crystallography of **7b**[9] confirmed this to be the α-L-anomer with the (*S*) stereochemistry at the amino acid centre, based on the known absolute configuration of the sugar starting material (Fig. 1). The X-ray of **7a** (unpublished results) also showed the α-L-anomer with the opposite stereochemistry at the amino acid centre.

Selective removal of the *N*-trifluoroacetate proved difficult as the amide was resistant to mild base hydrolysis (potassium carbonate, methanol) whereas under strongly basic conditions (sodium hydroxide or sodium methoxide) partial removal of the pivaloyl groups was seen. Successful deprotection was achieved by sodium borohydride reduction of the (*R*) diastereomer **7a** to **8**. However, the corresponding (*S*) diastereomer was resistant to sodium borohydride reduction, consistent with the steric crowding seen in the X-ray structure (Fig. 1) preventing access of the reducing agent. The amine **8** was then coupled to L-BOC-tyrosine. Removal of the pivaloyl groups with sodium methoxide caused hydrolysis of the methyl ester as well as epimerisation of one of the amino acid stereocentres. After deprotection, the diastereomers **9a** and **9b** were separated by reverse-phase preparative HPLC. Amino acid analysis showed that both diastereomers contained L-tyrosine, thus indicating that the epimerisation had occurred at the α-stereocentre of the *C*-glycosyl amino acid.[10]

The entire synthetic sequence was repeated using D-arabinose as the starting material, to give the diastereomers

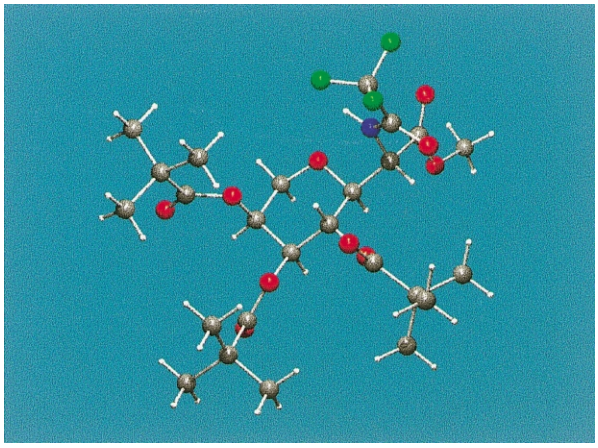

Figure 1. A view of the glycoside **7b** created with PLATON and POVRAY. Disordered atoms with lower site occupancies are omitted for clarity.

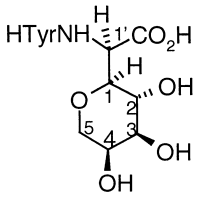

9a

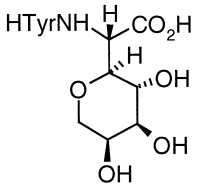

9b

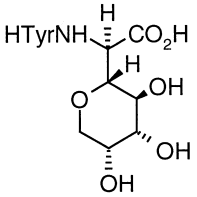

10a

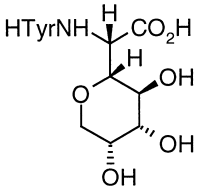

10b

Table 1. Inhibition of *S. aureus* YRS

Compound	Stereochemistry at C1′	Sugar ring		IC_{50} (nM)
1	(*S*)		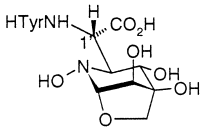	2.0
3	(*S*)		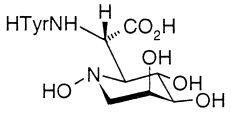	1.2
9a	(*R*)	α-L-Arabinose	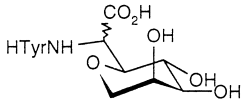	260
9b	(*S*)	α-L-Arabinose		100
10a	(*R*)	β-D-Arabinose	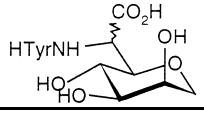	NI[a]
10b	(*S*)	β-D-Arabinose		NI

[a]NI = no inhibition at 3 μM.

10a and **10b.** The pyranosyl analogues **9a**, **9b**, **10a** and **10b** were evaluated as inhibitors of *Staphylococcus aureus* tyrosyl tRNA synthetase (YRS), in an aminoacylation assay.[11] As can be seen from Table 1, the L-arabinose-derived diastereomer **9b** was a potent inhibitor of bacterial YRS with an IC_{50} value of 100 nM. The epimer **9a** was less potent, with an IC_{50} of 260 nM. In contrast, no inhibition was observed for either of the diastereomers **10a** or **10b** derived from D-arabinose. The pyran **9b**, is thus an inhibitor of YRS with the preferred stereochemistry around the sugar ring, corresponding to **3** in which the hydroxylamine is directly replaced by oxygen. By comparison to compound **3**, the more active diastereomer **9b** was inferred to have the (*S*) stereochemistry at C1′. Compound **9b** was also tested against mammalian YRS and showed no inhibition up to 3 μM indicating that the bacterioselectivity seen in the hydroxylamine series has been retained.

In conclusion, we have shown that a synthetic analogue of SB-219383 in which the hydroxylamine-containing ring is replaced by a pyranose sugar is a stereoselective and bacterioselective inhibitor of tyrosyl tRNA synthetase. These results facilitate the further development of SARs of this series by allowing more ready synthetic access to postulated inhibitory analogues.

Acknowledgements

The authors would like to thank D. O'Brien and C. Seaman for 2D-NMR experiments.

References and Notes

1. Walker, G.; Brown, P.; Forrest, A. K.; O'Hanlon, P.; Pons, J. E. In *Recent Advances in the Chemistry of Anti-Infective Agents*; Royal Society of Chemistry: London, 1993; p 106.
2. Stefanska, A. L.; Coates, N. J.; Mensah, L. M.; Pope, A. J.; Ready, S. J.; Warr, S. R. *J. Antibiot*. **2000**, *53*, 345.
3. Houge-Frydrych, C. S. V.; Readshaw, S. A.; Bell, D. J. *J. Antibiot*. **2000**, *53*, 351.
4. Berge, J. M.; Broom, N. J. P.; Houge-Frydrych, C. S. V.; Jarvest, R. L.; Mensah, L.; McNair, D. J.; O'Hanlon, P. J.; Pope, A. J.; Rittenhouse, S. *J. Antibiot*. **2000**, *53*, 1282.
5. Berge, J. M.; Copley, R. C. B.; Eggleston, D. S.; Hamprecht, D. W.; Jarvest, R. L.; Mensah, L. M.; O'Hanlon, P. J.; Pope, A. J. *Bioorg. Med. Chem. Lett*. **2000**, *10*, 1811.
6. Postema, M. H. D. In *C-Glycoside Synthesis*; Rees, C. W., Ed.; CRC Press Inc.: Boca Raton, 1995; pp 1–63.
7. Simchen, G.; Pürkner, E. *Synthesis* **1990**, 525.
8. Oesterle, T.; Simchen, G. *Liebigs Ann. Chem*. **1987**, 687.
9. X-ray crystal structure determination of **7b**. Crystals were grown via the evaporation of an ethanol solution at reduced pressure. Crystal data: colourless prism, 0.59×0.38×0.28 mm;

$C_{25}H_{38}F_3NO_{10}$, $M_r = 506.28$, orthorhombic, $P2_12_12_1$ (no. 19), $a = 11.879(5)$, $b = 16.504(7)$, $c = 32.737(13)$ Å, $V = 6418(5)$ Å^3, $Z = 8$, $D_x = 1.179\ Mg\ m^{-3}$, μ(Mo Kα, $\lambda = 0.71073$ Å) = 0.101 mm^{-1}. Data collection: Nonius CAD4 diffractometer, FR591 rotating anode generator, graphite monochromator, 223 K, $\theta_{max} = 39.98°$, $\omega/2\theta$ scans, $N_{ref} = 5058$, $N_{uniq} = 4696$. Data reduction: corrections for Lorentz and polarization effects; decay correction, 4 standard reflections, maximum variation = 6.4%; $R_{int} = 0.088$. Solution and refinement: SHELXTL V5.10 IRIX package; direct methods; full-matrix least-squares refinement on F^2; disordered trifluoro and *t*-butyl groups modelled with partial occcupancy sites, coordinates and anisotropic displacement parameters refined for the non-hydrogen atoms (lower occupancy disordered atoms isotropic); hydrogen atoms in idealised positions, riding or as rigid rotating groups, with isotropic atomic displacement parameters which were an appropriate multiple of U_{eq} for the bonded atom; $N_{ref} = 4541$, $N_{par} = 704$, R1 [3162 data with $I > 2\sigma(I)$] = 0.074, wR2 (all data) = 0.133, S = 1.071; $\Delta\rho_{min} = 0.17$ e Å^{-3}, $\Delta\rho_{max} = 0.28$ e Å^{-3}; extinction coefficient = 0.0020(7). Crystallographic data for this structure has been deposited with the Cambridge Crystallographic Data Centre. Copies of the data can be obtained, free of charge, on application to the Director, CCDC, 12 Union Road, Cambridge, CB2 1EZ, UK (Fax: +44-(0)1223-336033 or e-mail: deposit@ccdc.cam.ac.uk).

10. All compounds were characterised by 400 MHz ^{1}H NMR, using 2D techniques where necessary. Comparison of ^{1}H NMR (D_2O) chemical shifts (ppm) and coupling constants (Hz) between compounds **3**,[5] **9a** and **9b** is shown below.

11. Brown, P.; Mensah, L. M.; O'Hanlon, P. J.; Osborne, N. F.; Pope, A. J.; Richardson, C. M.; Walker, G. *Bioorg. Med. Chem.* **1999**, *7*, 2473.

Examples of chemical shifts (ppm) and coupling constants (Hz) for compounds **3**, **9b** and **9a**

H	**3**	**9b**	**9a**
1	3.18 (dd, $J = 10.1, 1.1$)	3.87 (dd, $J = 10.0, 2.0$)	2.68, (dd, $J = 9.9, 1.5$)
2	3.4 (bt, $J = 9.8$)	3.62 (br.t, $J = 9.7$)	3.0 (bt, $J = 9.5$)
3	3.55 (dd, $J = 9.7, 3.5$)	3.77 (dd, $J = 9.5, 3.3$)	
4	4.01 (ddd, J ca. 4.9, 1.5, 1.5)	4.05, br.t (J ca. 3)	
5ax	2.83 (dd, $J = 11.8, 1.2$)	3.70 (br d, $J = 12.7$)	
5eq	3.34 (dd, $J = 11.7$, ca.3)	3.97 (dd, $J = 12.8, 2.0$)	
1′	4.82 (d, $J = 1.0$)	4.91 (d, $J = 1.9$)	4.65 (d, $J = 1.5$)